

X-ray reflectivity study of solution-deposited ZrO₂ thin films on self-assembled monolayers: Growth, interface properties, and thermal densification

K.A. Ritley, K-P. Just, F. Schreiber,^{a)} and H. Dosch

Max-Planck-Institut für Metallforschung, Heisenbergstrasse 1, D-70569 and Institut für Theoretische und Angewandte Physik, Universität Stuttgart, D-70550, Stuttgart, Germany

T.P. Niesen and F. Aldinger

Max-Planck-Institut für Metallforschung and Institut für Nichtmetallische Anorganische Materialien, Pulvermetallurgisches Laboratorium, Heisenbergstrasse 5, D-70569 Stuttgart, Germany

(Received 7 February 2000; accepted 31 August 2000)

Thin films of ZrO₂ were deposited from aqueous solution on Si(100) substrates precovered by functionalized alkyltrichlorosilane self-assembled monolayers (SAMs). The interface structure, thermal stability, and densification of these films in the temperature range from room temperature to 750 °C in vacuum were measured using *in situ* x-ray reflectivity. The growth rate is a nonlinear function of time in solution, with a pronounced nonuniformity during the first 30 min. The as-deposited films exhibit about 3-nm roughness and a density below that of bulk ZrO₂. Measurements in vacuum reveal decreasing film thickness, increasing film density, and decreasing roughness upon annealing up to 750 °C. The densification saturates at the highest measured temperatures, presumably following evaporation of residual contaminants from the aqueous synthesis procedure. Above 200 °C the SAM/ZrO₂ interface began to deteriorate, possibly due to interdiffusion. The ZrO₂ film structure obtained at the highest annealing temperatures persisted upon cooling to room temperature, and there was no visible evidence of stress-induced microstructural changes, such as peeling or cracking.

I. INTRODUCTION

Recent technological demand for thin films of metal oxides like ZrO₂ in applications such as oxygen sensors, high refractive-index optical coatings, and laser mirrors has spurred the development of synthesis techniques based on chemical processes, such as precipitation from aqueous solution and sol-gel,^{1,2} rather than physical ones, such as sintering and molecular beam deposition.^{3,4} Advantages of the chemical synthesis routes include low cost, suitability at low temperatures, uniform coverage, and the possibility of coating nonflat surfaces. Of the chemical synthesis techniques, a promising new method is precipitation from an aqueous precursor solution at temperatures below 100 °C onto a surface covered by an ordered organic array of functional groups, a technique which has been dubbed “biomimetic” inasmuch as it replicates the biological mechanisms for ceramic synthesis at low temperature.^{5,6} Self-assembled monolayers (SAMs) provide such an organic surface onto which ad-

ditional adsorbates can be anchored.^{7,8} Thin films of ZrO₂ and Y₂O₃-doped ZrO₂,⁹ Y₂O₃,¹⁰ SnO₂,¹¹ ZnO,¹² TiO₂,¹³ and V₂O₅^{14,15} have thus far been prepared using this technique, and they have been characterized at room temperature via transmission electron microscopy (TEM), x-ray diffraction, and atomic force microscopy.^{9,16} Studies of the temperature dependence of the thin film and interface properties have been less commonly undertaken.^{2,17,18}

In the present paper the results of temperature-dependent x-ray reflectivity measurements of such ZrO₂ thin films on SAMs are reported. This nondestructive technique provides microscopic information about the roughness, density profile, and thickness of the layers that compose the thin film, and it offers advantages over ellipsometry in that precise information about the properties of buried layers can be obtained. With the appropriate environmental chamber it can be applied to samples in vacuum at high temperature. Although not undertaken in the present work, x-ray scattering techniques can also be applied *in situ* during growth, thus making it possible to study the structural development of monolayers in real time.¹⁹

^{a)}Address all correspondence to this author.
e-mail: fschreib@dxray.mpi-stuttgart.mpg.de

This paper is organized as follows. First, the thin-film preparation is discussed, followed by a brief description of the x-ray reflectivity measurements and how the data analysis yields the layer thickness, density, and roughness. The results of room-temperature, temperature-dependent, and time-dependent measurements are presented next, followed by results that address the thin-film stability after thermal cycling.

II. EXPERIMENTAL

A. Sample preparation

The substrates employed in this work were 10 × 10 mm single-crystal Si(100) substrates cleaned and oxidized using Piranha solution (H₂SO₄:H₂O₂ = 7:3) at 80 °C and dried in argon. The subsequent film preparation sequence consisted of two general steps, SAM preparation and ZrO₂ growth. The completed SAM layer, shown in Fig. 1, consists of siloxane-anchored (CH₂)₁₆ hydrocarbon chains with SO₃H endgroups. This SAM structure was formed spontaneously on the wafer surface

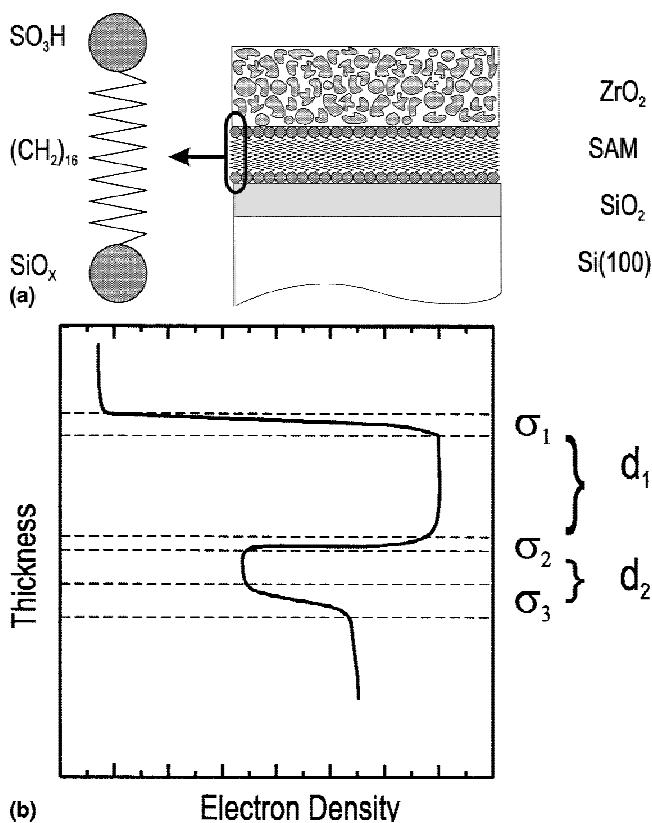


FIG. 1. (a) Cross section of the ZrO₂ thin films prepared by deposition from aqueous solution on SAM-covered Si substrates, showing the buried SAM interface; (b) the schematic of the electron-density profile of the thin films, showing the roughness d_j and roughness σ_j for each layer j .

by dipping the wafers into a dicyclohexyl solution containing 1% (by volume) of trichlorosilylhexadecane thioacetate [Cl₃Si-(CH₂)₁₆-S-C(O)CH₃] at room temperature for 5 h, followed by washing with chloroform to remove excess surfactant. In order to convert the thioacetate to a sulfonate (-SO₃H) functionality the wafers were immersed in an aqueous persulfate oxidant (2KHSO₅ · KHSO₄ · K₂SO₄, “oxone”) for a minimum of 4 h at room temperature. Details about the SAM synthesis have been reported elsewhere.²⁰

ZrO₂ thin films were deposited on the SAM-terminated Si surface in the following way. The SAM-bearing substrates were immersed in 10-ml aliquots of aqueous solutions of 4-mM zirconium sulfate/0.4 N HCl and kept in a constant-temperature oil bath set at 70 °C (SAM-coated side up). After the desired time had elapsed, the wafers were removed, rinsed three times in de-ionized water, and cleaned ultrasonically for 30 min before drying with a stream of dry argon gas. Full details of the film growth are published in Ref. 16.

The samples reported in this paper include bare and SAM-terminated Si wafers as well as ZrO₂ films obtained by maintaining the substrate in solution for 1 h, 2 h, and 4 h, respectively (hereafter referred to as 1H, 2H, and 4H). A second series of samples was prepared later to address the ZrO₂ thickness variability, which includes samples in solution for 30 min and 4 h, as well as a 4-h sample in which a fresh precursor solution was used in four successive depositions of 1 h each (referred to as 30MB, 4HB, and 4 × 1HB).

In addition to the x-ray reflectivity measurements, Rutherford backscattering spectroscopy (RBS) using 3-MeV He²⁺ ions was used to characterize the chemical purity of some of the films before annealing (sample 4H) and after annealing (samples 30MB, 4HB, and 4 × 1HB).

B. X-ray reflectivity: principles

The x-ray reflectivity scheme is shown in Fig. 2. A monochromatic, highly collimated x-ray beam with wavelength λ hits the sample surface at angle α . For

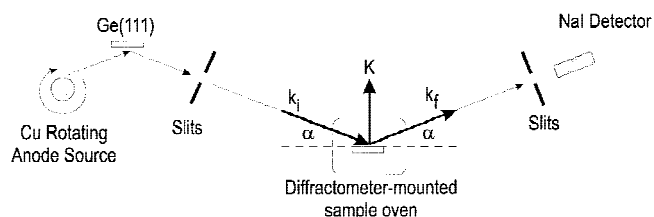


FIG. 2. Sketch of the specular x-ray reflectivity measurement scheme, showing the definition of the incident and exit angle α with respect to the sample surface, and the incident (k_i), reflected (k_f), and net ($k = k_f - k_i$) x-ray momentum vectors.

specular reflectivity, the momentum transfer q is perpendicular to the surface, the incident angle equals the exit angle, and therefore

$$q = \frac{4\pi}{\lambda} \sin\alpha \quad . \quad (1)$$

For a single interface, the reflectivity is well described by the Fresnel laws of classical optics.²¹ Total external reflection occurs below the critical angle α_c ; above α_c the reflectivity decays rapidly, approaching approximately $1/\alpha^4$ for large angles ($\alpha \gg \alpha_c$).

The x-rays are scattered by changes in the index of refraction n_j of the layers which compose the film (in the present case, the index j denotes the ZrO₂ layer, the SAM interlayer and the Si substrate; see Fig. 1), where

$$n_j = 1 - \delta_j + i\beta_j \quad , \quad (2)$$

with

$$\delta_j = r_e \lambda^2 \rho_j / 2\pi \quad , \quad (3)$$

and

$$\beta_j = \lambda \mu_j / 4\pi \quad . \quad (4)$$

$r_e = 2.818 \times 10^{-13}$ cm is the classical electron radius and μ_j is the mass absorption coefficient.

In the case of a layered system, the scattering from several interfaces has to be taken into account. This is done rigorously in the recursive approach of Parratt,^{21–23} where the ratio of the reflected and transmitted field amplitudes is calculated from

$$r_{j,j-1} = a_{j-1}^4 \frac{r_{j,j+1} + F_{j-1,j}}{r_{j,j+1} F_{j-1,j} + 1} \quad , \quad (5)$$

with

$$a_j = \exp(-iq_j d_j / 2) \quad , \quad (6)$$

$$F_{j-1,j} = \frac{q'_{j-1} - q'_j}{q'_{j-1} + q'_j} \exp[-q_{j-1} q_j \sigma_{j-1,j}^2 / 2] \quad , \quad (7)$$

and

$$q'_j = (q^2 - q_{c,j}^2 + 8\pi i \mu_j / \lambda)^{1/2} \quad , \quad (8)$$

where $q_{c,j}$ is the momentum transfer at the critical angle $\alpha_{c,j} = (2\delta_j)^{1/2}$. Eq. (5) is solved iteratively. Gaussian roughness is taken into account by the exponential factor in Eq. (7). The Parratt formalism automatically includes multiple scattering and refraction effects. The parameters that describe the thin film are obtained by fitting the data to Eq. (5). The layer thicknesses d_j determine the oscillation period [Eq. (6)], the interface roughnesses σ_j affect the damping of the oscillations [Eq. (7)], and electron densities ρ_j and absorption coefficients μ_j determine the critical edge [Eq. (8)] as well as the amplitude of the

oscillations. We note that the inclusion of roughness as done here in Eq. (7) is rigorously correct only for roughnesses much smaller than the individual layer thicknesses. However, because in this paper the relative changes are more important than the absolute numbers, the conclusions are not affected.

C. X-ray reflectivity: experimental details

The temperature-dependent x-ray reflectivity measurements were carried out on a 6-circle diffractometer furnished with Cu K_{α1} x-rays from a Siemens 18-kW generator. This system is equipped with a Ge(111) monochromator and has slits adjusted to provide an out-of-plane resolution of $\Delta q/q = 3 \times 10^{-4}$. The diffractometer is configured with computer-controlled arcs and translation stages, capable of positioning the sample laterally (to within 0.001 mm) and angularly (to within 0.001°) with respect to the x-ray beam. A schematic diagram of the setup is shown in Fig. 2.

A vacuum-pumped sample stage was used for *in situ* temperature-dependent reflectivity measurements. This stage, which sits atop the goniometer, is a turbomolecular-pumped vacuum chamber capable of reaching 1×10^{-6} mbar or below, with Kapton sidewalls that provide a large entrance and exit aperture for x-ray measurements. The sample heater consists of a resistively heated W filament behind a Ta plate, upon which the samples and a thermocouple are both securely affixed using spot-welded Ta wires, assuring good thermal contact at all temperatures.

The samples were each heated to the desired temperature, the alignment of the x-ray beam was adjusted and verified by performing “rocking curves” through the specular intensity, then the intensity of x-rays specularly reflected from the surface were recorded as a function of incident angle. Additionally, scans of the x-ray intensity offset from the specular condition ($2\theta/2 = \theta \pm \delta\theta_0$, with $\delta\theta_0 = 0.1^\circ$) were made, in order to correct the data for diffuse scattering.

III. RESULTS AND ANALYSIS

A. Characterization of as-deposited films

The reflectivity data for sample 2H, as well as for a bare and SAM-covered Si substrate, appear in Fig. 3 and the fitting results for samples 1H, 2H, and 4H appear in Table I. The bare Si substrate shows a smooth decay in intensity and the SAM-covered substrate shows low-intensity oscillations visible at higher angles. The ZrO₂-covered films show these same features but superimposed with high-intensity oscillations at low angles. Although the Si is covered by an amorphous silicon oxide layer, considerations of interfacial roughness and the contrast in index of refraction render thin-film oscilla-

tions from the Si oxide, if any, below the level of detectability for the present experimental conditions, as discussed in Ref. 24.

The measured ZrO₂ electron density, approximately $0.7 \times 10^3 \text{ nm}^{-3}$, is smaller than the bulk value of $1.3 \times 10^3 \text{ nm}^{-3}$ by nearly a factor of two, suggesting that the as-deposited films have significant intergrain contamination with low electron density or open volume defects. This issue is addressed in greater detail in Sec. III. B. The ZrO₂ roughness is found to be approximately 3 nm, which is within the range reported in recent atomic force microscopy studies of similar samples.¹⁶

The x-ray reflectivity measurements also provide information about the evolution of film thickness during growth from the aqueous solution, by comparing the as-deposited film thickness and roughness with the time each substrate was maintained in solution. The data, shown in Fig. 4, exhibit a negative curvature; that is, the growth rate decreases with time, with a strongly pronounced effect during the first 30 min in solution. This behavior is as expected, due to the loss of ZrO₂ from the precursor solution, and it is consistent with the reported metastability of the precursor solution, as reported by Agarwal *et al.*⁹ The decreasing growth rate is further confirmed by the thickness comparison between a

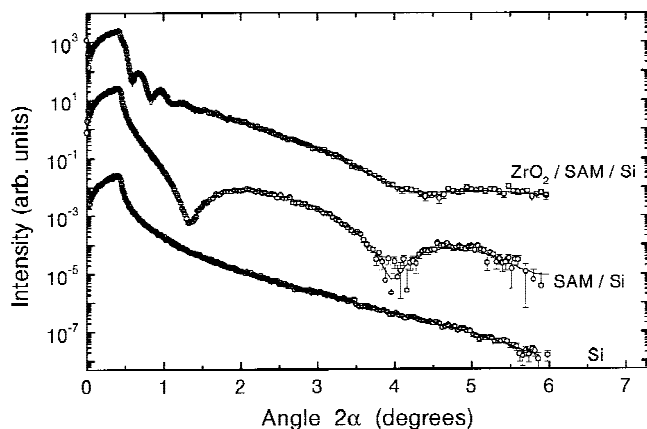


FIG. 3. Measured and normalized x-ray reflectivity curves for a bare Si substrate, a SAM-terminated Si substrate, and a ZrO₂//SAM//SiO₂//Si thin film with 26.8 nm ZrO₂ (sample 2H). The curves have been offset for clarity. The solid lines are fits to the data using the Parratt formalism described in the text. The maximum angle of 7° corresponds to an out-of-plane momentum transfer of $q = 0.5 \text{ \AA}^{-1}$.

ZrO₂ thin film prepared by four successive immersions of 1 h each in fresh solution (sample 4 × 1HB, 74 nm), with a film prepared by continuous immersion for 4 h (sample 4HB, 43 nm); the former sample has almost four times the thickness as the sample in solution for 1 h. All data clearly support the notion of a less than linear increase of the thickness with time in the present growth regime.

The thickness of the SAM layer determined by fitting is approximately 2 nm for a fully covered substrate, as expected from structural considerations and in agreement with ellipsometric measurements on similar samples.¹⁶ The electron density is approximately $0.3 \times 10^3 \text{ nm}^{-3}$ and is typical of that for thin films of crystalline hydrocarbons.

RBS measurements on sample 4HB confirm that the density of the ZrO₂ layer is below the bulk value, and these indicate the as-grown films contain an overabundance of oxygen as well as chlorine and sulfur. The latter two species are not unexpected, based on the S- and Cl-containing composition of the aqueous precursor solution. Although the measurements were incapable of separately resolving S and Cl, or detecting their specific depth distribution, rough values are estimated as 1×10^{16} and $0.4 \times 10^{16} \text{ at/cm}^2$, respectively. If these contaminants were present as thin films, this corresponds to effective thicknesses of 2.5 nm and 1.0 nm, respectively. These values are greater than those expected from the SAM layer alone and are due to incorporation of residual material from the aqueous precursor solution.¹⁷

Finally, the as-deposited films were found to be stable in air at room temperature over long time scales. Reflectivity measurements performed after several months were identical to those performed immediately following sample preparation.

B. Temperature-dependent studies

Reflectivity measurements were subsequently performed as a function of temperature and time at a given temperature. In all cases information about the ZrO₂ layer, which appears as short-period, high-intensity oscillations in the low-angle region of the reflectivity curve (see Fig. 3) could be obtained with high precision. Precise measurement of the SAM layer could in principle be achievable with sufficiently long counting time; how-

TABLE I. Values of the parameters obtained by fitting x-ray reflectivity data for the as-deposited films.^a

Sample	Thickness ZrO ₂ (nm) ± 0.5	Roughness ZrO ₂ (nm) ± 0.1	Electron density ZrO ₂ ($\times 10^3 \text{ nm}^{-3}$) ± 0.03	Thickness SAM (nm) $\sigma_2 \pm 0.1$	Roughness SAM (nm) ± 0.1	Electron density SAM ($\times 10^3 \text{ nm}^{-3}$) ± 0.02
1H	19.9	2.7	0.76	1.9	0.54	0.28
2H	26.8	2.8	0.81	1.4	0.67	0.29
4H	37.4	3.8	0.76	1.6	0.56	0.31

^aThe reported uncertainty is based on a 95% confidence interval for variations of the chi-square (χ^2) of the fit. The roughness of the substrate was below 0.3 nm.

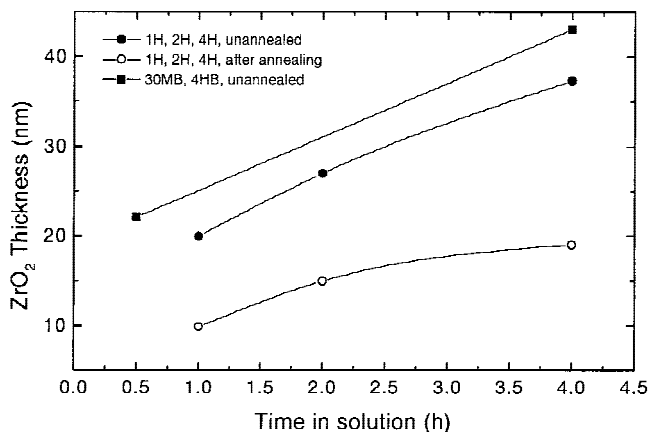


FIG. 4. The thickness of the as-deposited films as a function of the deposition time of the wafer in solution. Extrapolation of the linear trend to zero shows the highly nonuniform growth rate during the initial stages of deposition. This is further demonstrated by the large thickness (74 nm, data point not shown) of sample $4 \times 1\text{HB}$, grown by four successive immersions for 1 h each in fresh solution (see text). The solid lines are a guide to the eye.

ever, to minimize time-dependent effects the measurements were restricted to typically 1 or 2 h per temperature. For temperatures below 400 °C the qualitative temperature-dependent behavior of the SAM layer is still readily inferred although at some sacrifice to quantitative precision. Due to disordering of the SAM interlayer at higher temperatures the measured signal is not sufficient for quantitative analysis, as discussed in detail below.

1. Behavior of the ZrO₂ layer

The temperature-dependent reflectivity for sample 1H is shown in Fig. 5, and the results of fitting the reflectivity curves for all samples appear in Fig. 6–9. Two important features are immediately apparent. First, the film thickness for all films initially decreases linearly with temperature, for the time scale of the present experiment (1–2 h per measurement). This decrease is accompanied by a corresponding increase in film density. For sample 4H, this decrease persists until about 400 °C, above which the thickness remains almost constant. For samples 1H and 2H, the thickness decrease persists until the highest measured temperature (500 and 600 °C, respectively), but the final density is below bulk density. These results are consistent with earlier TEM investigations that compare as-deposited and annealed films, in which shrinkage of 46% was typical.¹⁷

Second, the initial rate of ZrO₂ thickness decrease shown in Fig. 6(a) is sample dependent. For samples 1H, 2H, and 4H the initial densification rates are $-0.021 \pm 0.001 \text{ nm}/^\circ\text{C}$, $-0.032 \pm 0.001 \text{ nm}/^\circ\text{C}$, and $-0.048 \pm 0.001 \text{ nm}/^\circ\text{C}$, respectively. As Fig. 6(b) shows, however, the normalized thickness change (thickness divided by

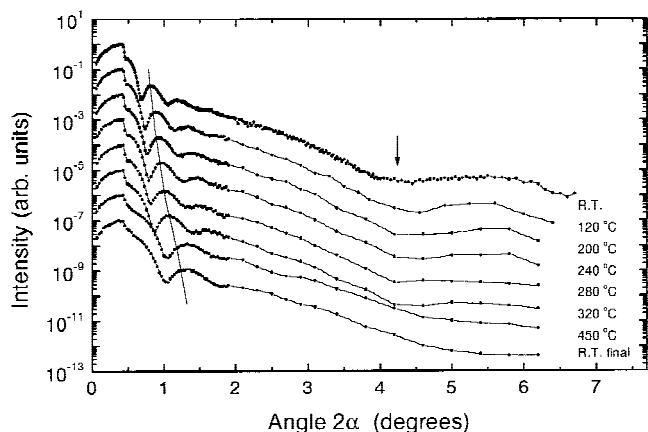


FIG. 5. The reflectivity profiles for sample 1H measured at different temperatures. The curves have been normalized to a maximum peak intensity of one and successively offset by a factor of 10 for clarity. The solid lines are a guide to the eye, showing the wavelength increase with increasing annealing temperature of the short-period oscillations, due to shrinkage of the ZrO₂ layer thickness. The arrow indicates the start of the intensity oscillation due to the SAM. Above about 400 °C this feature does not appear well defined during the typical 1–2 h scanning times, due to structural disordering of the SAM interlayer (see text).

the thickness of the as-deposited films) is the same for all samples (approximately $-1.2 \times 10^{-3} /^\circ\text{C}$), suggesting that the densification is a volume-driven (“bulk”) process as opposed to a surface-driven process, which would yield the same *absolute* rates of change for different thicknesses. The ZrO₂ electron density increases with temperature, as shown in Fig. 7(a), reaching approximately the expected bulk value for the sample annealed at the highest temperature. The ZrO₂ coverage, defined by the product of density and thickness, is shown in Fig. 7(b), and should be a constant function of temperature if the film composition remains fixed.

Equal rates of normalized ZrO₂ thickness change [Fig. 6(b)] for all samples are expected if the thickness reduction during densification primarily involves compaction of as-deposited material via the elimination of free volume defects, or possibly the loss of mass via desorption of light-electron-density contaminants (for example, O, S, and Cl). The general saturation of the coverage observed at temperatures above 400 °C [Fig. 7(b)] suggests that the loss of contaminants is saturated and only the elimination of voids is taking place. Further measurements, such as RBS studies of thin-film composition for each of the annealing temperatures, may be required to estimate the magnitude of these two separate effects.

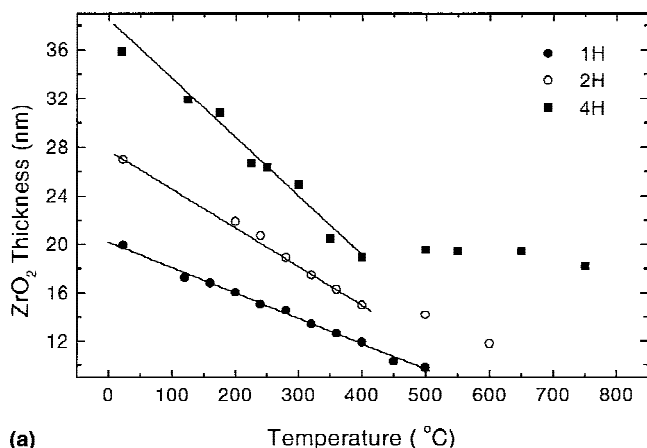
As Fig. 8 shows, the densification process is accompanied by a decrease in roughness. Interestingly, for all samples the initial roughness scales approximately with the thickness, and the relative change in roughness with temperature is similar. The evolution of thin-film rough-

ness with thickness has been studied theoretically and experimentally in a variety of different thin-film systems,²⁵ but the limited data set in the present experiment does not permit detailed conclusions about the growth mode to be drawn.

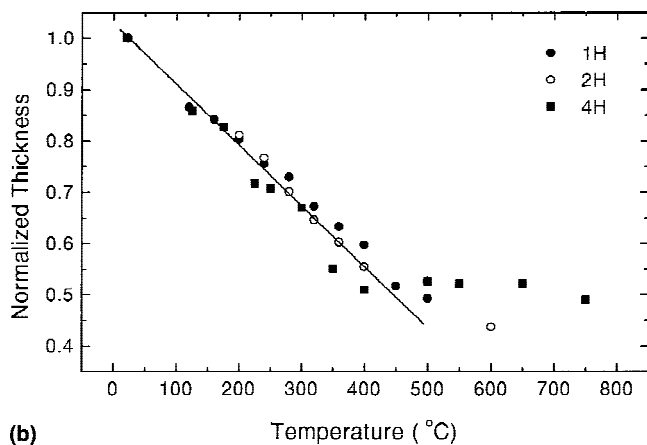
Finally, we note that a recent study of ZrO₂ prepared by sol-gel techniques reported different densification kinetics in two temperature regimes, above and below 300 °C.² However, the samples in that study were maintained at each temperature for 15 min. and then subsequently cooled for measurement, in contrast to the present work in which high temperature was maintained continuously (>1 h) for each measurement. The time dependence of the densification process is reported in greater detail in Sec. III. C.

2. Behavior of the SAM interlayer

Due to the low measured intensity at higher angles during the 1–2-h reflectivity measurements, precise quantitative information about the SAM layer is difficult



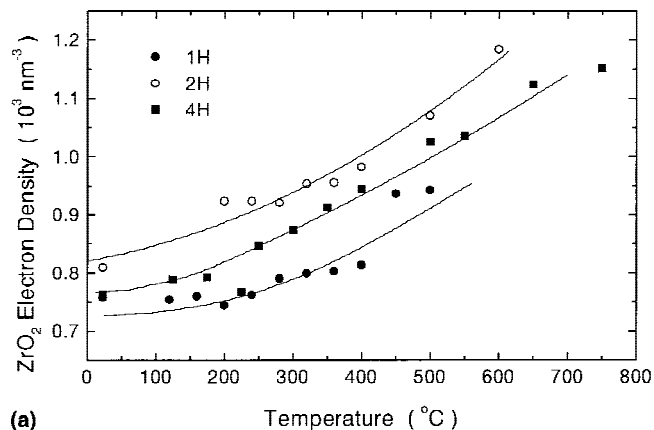
(a) Temperature (°C)



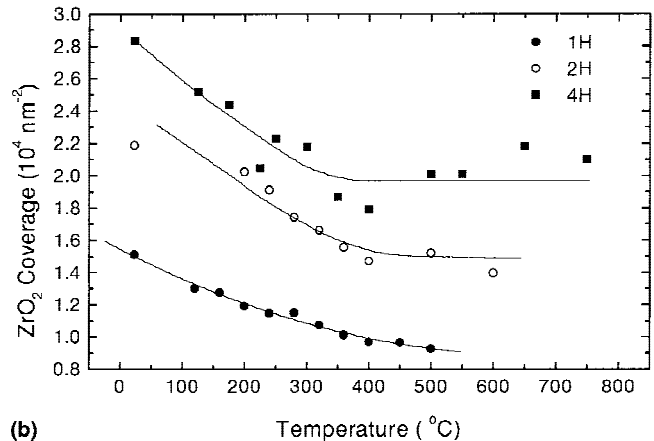
(b) Temperature (°C)

FIG. 6. (a) The temperature-dependence of the ZrO₂ thickness. (b) The ratio of the ZrO₂ thickness at temperature T to the value measured at room temperature, showing the same temperature dependence for all samples during initial densification. The solid lines are a guide to the eye.

to obtain. Above 400 °C the measured intensity falls below that required to obtain reliable values by fitting, and thus we report values of the thickness and roughness only for temperatures below this.

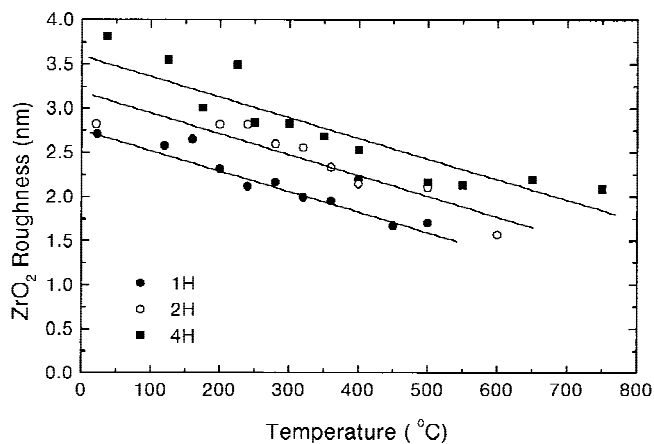


(a) Temperature (°C)



(b) Temperature (°C)

FIG. 7. (a) The temperature dependence of the electron density of ZrO₂. (b) The coverage of the ZrO₂ layer, defined by the product of the density and thickness. This quantity is expected to saturate at higher temperatures, if there is no loss of ZrO₂, once the densification is complete. The solid lines are a guide to the eye.



(a) Temperature (°C)

FIG. 8. Temperature dependence of the roughness of ZrO₂. The roughness of the as-deposited films scales with the film thickness, and the change in roughness with temperature is similar for all samples. The solid lines are a guide to the eye.

The SAM thickness decreases with temperature over the complete temperature range, as shown in Fig. 9, from which the depletion or decomposition of the SAM layer may be concluded. The depletion begins just above 200 °C and continues throughout the densification.

Unfortunately the experimental resolution is not sufficient to distinguish between two possibilities: (i) whether the SAM layers chemically decompose or (ii) whether they merely detach from the substrate and inter-diffuse. Shin *et al.*²⁶ have shown in TEM investigations of comparable TiO₂ thin films on SAMs that SAM decomposition was complete after 2 h at 400 °C in nitrogen, but no change in SAM thickness could be determined after 2-h annealing at 200 °C or 300 °C. (Note that no thickness decrease was found after annealing in air, which was explained by the growth of the SiO₂ layer compensating the thickness of the pyrolyzed organic layer.²⁶) Without covering the SAM by an oxide thin film, cleaving of the functionality (i.e., thioacetate) from the hydrocarbon chains was indicated after heat treatment at 250 °C for 30 min in vacuum, and significant loss of carbon was found at 400 °C.²⁶

The temperature stability of uncovered alkyltrichlorosilane on oxide-covered Si(100) has been measured recently by Kluth *et al.* using high-resolution electron energy loss spectroscopy.^{27–29} These authors have shown that this system exhibits short time stability in vacuum until approximately 430 °C, at which point chemical decomposition begins to occur via C–C bond cleavage. Further, it was shown that the siloxane head group remains attached to the surface until 830 °C. Assuming that the C–C thermal decomposition threshold for the SAM is essentially the same with and without a covering ZrO₂ layer, we conclude that interdiffusion and disordering at the interface is the dominating process in the deterioration of SAM interlayer.

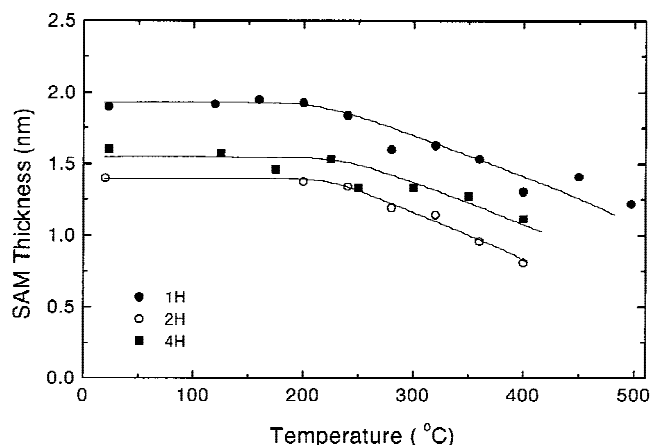


FIG. 9. The SAM layer thickness as a function of annealing temperature, which shows a gradual thickness decrease above about 200 °C. Above 500 °C information regarding the SAM layer could not be extracted from the reflectivity scans due to constraints of the data acquisition time. The solid lines are a guide to the eye.

C. Time-dependent measurements

During the densification study some measurements were taken at fixed temperature for longer times, to ascertain the time dependence of the densification process. The minimum time required to complete one reflectivity measurement per temperature, in addition to the time required to reach temperature, places a lower bound of about 1.5 h on the time resolution. For all samples prolonged annealing for several hours at fixed temperature resulted in a ZrO₂ thickness decrease of about 0.5 nm per hour, and this value was not strongly temperature dependent. Thus a slow densification continues at fixed temperature and long times, but the magnitude of the thickness change is not appreciable compared with that which occurs for successively higher temperatures. These results establish that any significant time-dependent effects must occur on a scale faster than the minimum 1.5 h required to complete a measurement, and that the above temperature-dependent results represent the thin-film properties after the completion of the short-time-scale processes.

D. Characterization after annealing

Final reflectivity measurements were performed again at room temperature following the temperature-dependent measurements. The layer thickness, density, and roughness retained the values measured at high temperature, showing the stability of the films following densification and apparently negligible effect of differential thermal expansion or stress development upon cooling.

To investigate possible changes in the crystallinity of the films following the vacuum annealing studies, high-angle (powder) x-ray diffraction measurements of some samples were performed prior to and subsequent to annealing. The results of these measurements showed the films to be essentially x-ray amorphous (i.e., no Bragg peaks were detected), with no significant change before or after annealing. The behavior of the sample crystallinity with vacuum annealing at temperatures above 750 °C is currently under investigation.³⁰

RBS measurements performed on sample 4H subsequent to annealing revealed a significantly reduced content of sulfur, approximately 0.5×10^{16} at/cm²; if it were present in a homogeneous layer, this would correspond to an effective thickness of 1.25 nm. This results most likely from the aqueous zirconium sulfate precursor solution employed for ZrO₂ synthesis. No Cl signal was detected, confirming the earlier suggestion that the densification involves stoichiometric changes to some extent.

Finally, there was no visible evidence of cracking or macroscopic deterioration of the film after annealing. Recent work on thin films of ZrO₂ deposited on glass sub-

strates by sol-gel methods, in contrast, reported cracking of the films due to high tensile stress induced during annealing,² which further reflects the strong microstructural dependence of the material properties.

IV. SUMMARY AND CONCLUSIONS

Thin films of ZrO₂ were prepared on SAM-covered Si substrates, via a room-temperature chemical synthesis technique involving an aqueous precursor solution. In situ x-ray reflectivity measurements during vacuum annealing provided a quantitative measurement of film thickness, roughness, and electron density. The as-deposited films were found to have an x-ray amorphous ZrO₂ layer with considerable open volume defects, offset from the substrate by a well-ordered SAM layer with small roughness. Measurements performed on films prepared with different deposition times reveal a growth rate that decreases with time and indicates sensitivity to the initial conditions of the precursor solution.

The temperature-dependent changes to ZrO₂ layers observed were an increase in density with temperature and a decrease in thickness, pointing to a volume-driven process due to scaling with the initial thickness. The SAM/ZrO₂ interface was found to steadily decompose with increasing temperature above 200 °C. Bulk x-ray-diffraction measurements show that the films remain x-ray amorphous after the present annealing procedure.

These results demonstrate the utility of in situ temperature-dependent x-ray reflectivity studies of thin films synthesized by aqueous solution chemistry, and they should further promote the understanding of the thermal behavior of organic-inorganic interfaces and metal oxide thin films, which are becoming increasingly important for technological applications.

ACKNOWLEDGMENTS

We thank B. Edinger for assistance with some of the measurements and M.R. DeGuire for useful discussions. We are grateful to D. Plachke (Max-Planck-Institut Stuttgart) for the RBS measurements. Partial financial support was provided by the Deutsche Forschungsgemeinschaft under grant AL 384/22-1/2.

REFERENCES

1. K. Bandyopadhyay and K. Vijayamohan, *Langmuir* **14**, 6924 (1998).
2. R. Brenier, C. Urlacher, J. Mugnier, and M. Brunel, *Thin Solid Films* **338**, 136 (1999).
3. C.R. Aita, M.D. Wiggins, R. Whig, C.M. Scanlan, and M. Gajdardziska-Josifovska, *J. Appl. Phys.* **79**, 1176 (1996); M. Ghanashyam Krishna, S. Kanakaraju, and K. Narasimha Rao, and S. Mohan, *Mater. Sci. Eng. B* **21**, 10 (1993).
4. M. Balog, M. Schieber, M. Michman, and S. Patai, *Thin Solid Films* **47**, 109 (1977).
5. S. Mann, in *Biomimetic Materials Chemistry*, edited by S. Mann (VCH Publishers, New York, 1996), pp. 1–40.
6. B.C. Bunker, P.C. Rieke, B.J. Tarasevich, A.A. Campbell, G.E. Fryxell, G.L. Graff, L. Song, J. Liu, J.W. Virden, and G.L. McVay, *Science* **264**, 48 (1994).
7. A. Ulman, *An Introduction to Ultrathin Organic Films: from Langmuir-Blodgett to Self-Assembly* (Academic Press, Boston, 1991).
8. A.H. Heuer, D.J. Fink, V.J. Larai, J.L. Arias, P.D. Calvert, K. Kendall, G.L. Messing, J. Blackwell, P.C. Rieke, D.J. Thompson, A.P. Wheeler, A. Veis, and A.I. Caplan, *Science* **255**, 1098 (1992).
9. M. Agarwal, M.R. DeGuire, and A.H. Heuer, *J. Am. Ceram. Soc.* **80**, 2967 (1997).
10. M. Agarwal, M.R. DeGuire, and A.H. Heuer, *Appl. Phys. Lett.* **71**, 891 (1998).
11. S. Supothina and M.R. DeGuire (unpublished).
12. M.R. DeGuire, T.P. Niesen, S. Supothina, J. Wolff, J. Bill, C.N. Sukenik, F. Aldinger, A.H. Heuer, and M. Rühle, *Z. Metallkd.* **89**, 758 (1998).
13. H. Shin, R.J. Collins, M.R. DeGuire, A.H. Heuer, and C.N. Sukenik, *J. Mater. Res.* **10**, 692 (1995).
14. T.P. Niesen, J. Wolff, J. Bill, T. Wagner, and F. Aldinger, in *Advances in Science and Technology*, edited by P. Vincencini (Technical Publications, Florence, 1999) Vol. 20, pp. 21–34.
15. T.P. Niesen, J. Wolff, J. Bill, M.R. DeGuire, F. Aldinger, in *Organic/Inorganic Hybrid Materials II*, edited by L.C. Klein, L.F. Francis, M.R. DeGuire, and J.E. Mark (Mater. Res. Soc. Symp. Proc. **576**, Warrendale, PA, 1999) pp. 197–202.
16. A. Fischer, F.C. Jentoft, G. Weinberg, R. Schögl, T.P. Niesen, J. Bill, F. Aldinger, M.R. DeGuire, and M. Rühle, *J. Mater. Res.* **14**, 2464 (1999).
17. M. Agarwal, Ph.D. Thesis, Case Western Reserve University, Cleveland, OH (1997).
18. H.J. Shin, Y.H. Wang, U. Sampathkumaran, M.R. DeGuire, A.H. Heuer, and C.N. Sukenik, *J. Mater. Res.* **14**, 2116 (1999).
19. F. Schreiber, A. Eberhardt, T.Y.B. Leung, P. Schwartz, S.M. Wetterer, D.J. Lavrich, L. Berman, P. Fenter, P. Eisenberger, and G. Scoles, *Phys. Rev. B* **57**, 12476 (1998).
20. N. Balachander and C.N. Sukenik, *Tetrahedron Lett.* **29**, 5593 (1988); N. Balachander and C.N. Sukenik, *Langmuir* **6**, 1621 (1990); R.J. Collins and C.N. Sukenik, *Langmuir* **11**, 2322 (1995).
21. M. Tolan, *X-Ray Scattering From Solt-Matter Thin Films*, Springer Tracts in Modern Physics Vol. 148 (Springer, Berlin, 1999).
22. M. Deutsch and B.M. Ocko, *Encyclopaedia of Applied Physics* (Wiley, New York, 1998) Vol. 23, p. 479.
23. L.G. Parratt, *Phys. Rev.* **95**, 359 (1954).
24. R.A. Cowley, T.W. Ryan, *J. Phys. D* **20**, 61 (1987).
25. A. Pimpinelli and J. Villain, *Physics of Crystal Growth* (Cambridge University Press, Cambridge, 1998), and references therein.
26. H. Shin, Y. Wang, U. Sampathkumaran, M.R. DeGuire, A.H. Heuer, and C.N. Sukenik, *J. Mater. Res.* (in press).
27. G. Jonathan Kluth, Myung M. Sung, and Roya Maboudian, *Langmuir* **13**, 3775 (1997).
28. Myung M. Sung, G. Jonathan Kluth, Oranna W. Yauw, and Roya Maboudian, *Langmuir* **13**, 6164 (1997).
29. G.J. Kluth, M. Sander, M.M. Sung, and R. Maboudian, *J. Vac. Sci. Technol. A* **16**, 932 (1998).
30. K. Ritley, K-P. Just, F. Schreiber, T.P. Niesen, F. Aldinger, and H. Dosch, Proceedings of the 4th International Conference on Thin Film Physics and Applications (Shanghai, China, 2000).